Journal of Carcinogenesis
Covering Genesis to Therapeutics

Journal of Carcinogenesis, ISSN: 1477-3163
2025; Vol 24: Issue 9s, https://carcinogenesis.com/

Formulation and Evaluation of Imiquimod-Loaded Ethosomal Gel for Enhanced Topical Therapy of Skin Cancer

Bharti Choudhary[1*], Jitendra Banweer[2]

[1]School of Pharmaceutical Sciences, Sanjeev Agrawal Global Educational University, Bhopal 462022, Madhya Pradesh, India.

[2]School of Pharmaceutical Sciences, Sanjeev Agrawal Global Educational University, Bhopal 462022, Madhya Pradesh, India.

*Corresponding author:

Bharti Choudhary

School of Pharmaceutical Sciences,

Sanjeev Agrawal Global Educational University, Bhopal 462022, Madhya Pradesh, India

E-mail address: patelbharti90@gmail.com

ABSTRACT

Imiquimod doesn't dissolve or permeate the skin efficiently, limiting its topical application and causing localized discomfort and poor response. In ethosomal vesicles, imiquimod is easier to penetrate the skin, stays in the skin longer, is less toxic, and is more effective against skin cancer, particularly melanoma. A modified cold approach was used to make imiquimod ethosomal formulations. Using Box-Behnken Design, we optimized phospholipid, ethanol, and propylene glycol concentrations. The improved formulations' vesicle size, entrapment efficiency, flux, TEM, DSC, XRD, and chemical compatibility were examined. In vitro experiments included apoptosis (DAPI, flow cytometry), DNA fragmentation, colony formation assays, A375 melanoma and L929 fibroblast cell uptake and cytotoxicity, and Franz diffusion cell skin penetration. The gel's stability, histology, skin adhesion, and physicochemical characteristics were examined after mixing an improved ethosomal formulation (IMQ-ETH) with a carbopol gel. Improved ethosomal gel (IMQ-ETH) showed 87.47% entrapment efficacy, nanosized spherical vesicles (100 nm), and five times greater epidermal penetration than standard gel. The medicine penetrated deep into the skin and killed melanoma cells by boosting apoptosis and nuclear absorption, according to fluorescence imaging and in vitro experiments. The formulation improved Imiquimod's localized distribution and therapeutic efficacy, making it a potent topical skin cancer rival.

KEYWORDS: *Imiquimod, Ethosomes, Skin Cancer, Topical Delivery, Nanovesicular Systems, Cytotoxicity*

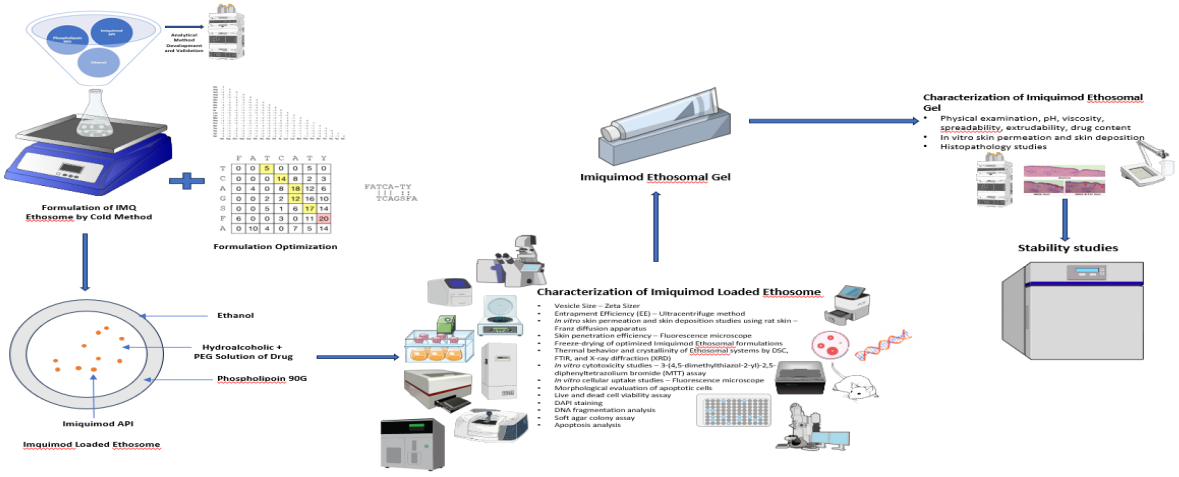

How to Cite: Bharti Choudhary, Jitendra Banweer., (2025) Formulation and Evaluation of Imiquimod-Loaded Ethosomal Gel for Enhanced Topical Therapy of Skin Cancer, *Journal of Carcinogenesis, Vol.24, No.9s,* 504-515.

1. INTRODUCTION

Skin cancer, encompassing both nonmelanoma and melanoma subtypes, continues to pose a significant global health challenge due to rising incidence and poor prognosis in metastatic forms. Conventional topical treatments, such as creams and gels, are often hindered by the stratum corneum barrier, which limits drug penetration, leading to inadequate local drug concentrations, reduced efficacy, and adverse effects.[1] This limitation is especially relevant for Imiquimod, an immune-response modifier used in basal cell carcinoma and actinic keratosis. While effective, imiquimod is hampered by poor solubility, inconsistent delivery, notable skin irritation, and dose variability—issues that can negatively affect patient compliance and therapeutic outcomes. [2, 3]

To circumvent these limitations, nanovesicular systems, particularly ethosomes, have emerged as promising drug delivery platforms. Ethosomes, first described by Touitou et al. in 1996, are deformable phospholipid vesicles containing high ethanol concentrations (20–45%) and water, enabling them to fluidize stratum corneum lipids and penetrate deeper skin layers. [4, 5] Ethanol not only enhances lipid fluidity ("ethanol effect") but also imparts flexibility to vesicles ("ethosome effect"), improving both permeation and vesicle deformation compared to conventional liposomes. [6]

Ethosomes outperform traditional liposomes in delivering both hydrophilic and hydrophobic compounds into the skin. For instance, ethosomal 5-aminolevulinic acid achieved 11–15× higher protoporphyrin IX accumulation than liposomes in porcine skin models, demonstrating substantially enhanced skin delivery. [7] In another study, ethosomal 5-fluorouracil showed six-fold better skin deposition, lower irritation, and improved anti-tumor performance compared to hydroethanolic solutions. [8]

This enhanced delivery approach has been successfully translated to anticancer treatments. For instance, preclinical models using ethosomal systems encapsulating sonidegib and cisplatin–imiquimod exhibited higher skin retention, increased bioavailability, and superior tumor suppression. [9, 10] Similarly, ethosomal delivery of berberine and evodiamine demonstrated potent melanoma cytotoxicity in vitro, confirming ethosomes' potential in oncology.[11] Another study highlighted curcumin ethosomal gels achieving high skin deposition and effective melanoma cell inhibition over 12 hours. [12]

Despite the robust evidence supporting ethosomes in dermal anticancer delivery, Imiquimod-loaded ethosomes are underexplored. Given imiquimod's therapeutic relevance and known drawbacks in traditional formulations, ethosomal encapsulation could markedly improve its solubility, skin deposition, therapeutic index, and reduce local side effects.

Accordingly, the present study aims to develop and evaluate Imiquimod-loaded ethosomal gels, focusing on particle characterization, skin permeation and retention, and in vitro cytotoxicity against melanoma models. We hypothesize that the ethosome-based gel will enable deeper dermal penetration, higher drug delivery, enhanced therapeutic efficacy, and reduced adverse effects, presenting a nanotechnology-driven strategy for advanced skin cancer therapy.

2. MATERIALS AND METHODS

We used pieces from several reliable sources in this investigation. Teva API India Ltd. provided Imiquimod API. Phospholipon 90G, propylene glycol, carbopol 934, PEG 400, mannitol, and crystal violet color were supplied by Fine Chem Pvt. Mumbai, India. Shri Maruti Chem Enterprise sent ethanol. Ltd. and Omkar Enterprises supplied concentrated hydrochloric acid. Rankem Chemicals made lactic acid. Central Drug House Pvt. Ltd. supplied methanol, isopropyl alcohol, and phosphate-buffered saline. Rhodamine 6G from Loba Chemie Ltd. and acridine orange/ethidium bromide, DAPI, FBS, DMEM, and agar from Thermo Fisher Scientific were fluorescent dyes. Finally, Jant Pharmacal Corporation sent us the DNA isolation kit (QIAamp).

Preparation of Imiquimod loaded ethosomes

Standard procedures for making a stable ethosomal formulation are difficult since imiquimod dissolves poorly in water and only slightly in ethanol. To avoid this, utilize co-solvents such polyethylene glycol 400 (PEG 400) and ethanol in a modified cold technique. These co-solvents increase imiquimod dissolution and stabilize the ethosomal vesicle. This cold approach encapsulates imiquimod in ethosomes, making it more soluble, trapping it, and improving skin penetration. This makes it a good topical drug delivery for actinic keratosis and basal cell carcinoma. [13] The required amount of Phospholipid 90G

was dissolved in propylene glycol and ethanol to generate the ethosomal formulation. Using magnetic stirring at room temperature (25–30°C), this combination became a clear and homogenous lipid solution. After the phospholipids dissolved, 0.5% Imiquimod—1/10th of Imiquimod Cream (5%), was added to the lipid phase. Further stirring for 20 minutes ensured that the drug was fully dissolved in the hydroalcoholic phase. Distilled water (qs to 100 ml) was heated to 30–35°C for the watery stage. We added this heated water phase to the lipid solution drop by drop while swirling with a magnetic stirrer at 700–1000 rpm. After 30–45 minutes, ethanol and water combined with phospholipids formed ethosomal vesicles on their own.16 Sonicating the dispersion with a probe for 3 minutes at 40% amplitude with 30-second pulses on and off to keep the temperature low reduced and uniformized the vesicles. The completed formula was stored at 4°C in sealed glass vials until further characterization. [14]

Experimental design

A screening was conducted to identify key parameters affecting stable ethosomal formulation. In Design-Expert® software (version 11), the Box-Behnken Design improved three significant independent variables: phospholipid 90G (A1), ethanol (A2), and propylene glycol (A3). The study examined 15 trial combinations for each element at three levels using the response surface approach. The dependent variables were Flu0078 (B3), entrapment effectiveness (B2), and vesicle size (B1). Formulation optimization employed a polynomial equation to represent how linear, interaction, and quadratic independent variable factors affected responses. [15]

Ethosome characterization

Using the Malvern Zetasizer (Malvern Instruments, Worcestershire, UK), ethosome formulations were measured for vesicle size, size distribution, and zeta potential at 25 ± 1 degrees Celsius. After diluting each sample with milli Q water, estimates were made three times. HPLC and ultracentrifugation techniques were used to determine the entrapment efficiency of ethosomal formulations. Transmission electron microscopy (TEM- Tecnai, G20, Philips Scientific) was employed to evaluate the morphological characteristics of ethosomes. [16] [17] [18]

In vitro investigations of skin permeability and deposition

Studies used Wister albino rats' excised abdominal skin for permeation experiments. Once sliced and separated, the skin was treated with isopropyl alcohol. Iquimod-loaded formulations were tested for skin permeation in vitro using a PermeGear Franz diffusion cell. Ethosomal formulations, comprising 0.5 mg imiquimod, were applied to the skin with ethanolic phosphate buffer in the receptor chamber. Samples were obtained at set times for HPLC analysis. Skin permeation parameters included permeability coefficient, enhancement ratio, flux, and cumulative medicine per unit area. Imiquimod's Kp and ER are measured in a skin permeation experiment. Washing, homogenizing, and sonicating the skin after 24 hours removes imiquimod. HPLC measures imiquimod after centrifuging and filtering the extraction solution. [19]

Efficiency of ethosomal systems skin penetration

Fluorescence microscopy measured Ethosome skin penetration. After treating rat abdomen skin with ethosome formulations including rhodamine 6G, it was washed and sliced thinly. A Rh6G hydroalcoholic solution was applied to the skin for comparison.[20]

Freeze-drying

The ethosome dispersion required grinding into a powder for FTIR, XRD, and DSC investigations. Mannitol was employed for cryoprotection following the lyophilization of unfilled-ETH and optimised Imoquimod- ethosomes loaded (IMQ-ETH). The formulations were initially subjected to freezing for 24 hours at -80°C. and thereafter stored at -20°C. The desiccated powder was preserved for subsequent research. [21] [22] [23]

In vitro cellular culture investigations

Cell culture

The Pune-based National Centre for Cell Sciences (NCCS) provided the human melanoma cell line (A375). At 37 °C, A375 cells were cultured in a CO2 incubator (New Brunswick Galaxy 170R, Eppendorf) with 5% CO2, 10% FBS, and 1% antibiotic-antimycotic (100X) solution. [24]

In vitro cytotoxicity evaluation

Imiquimod, Blank-ETH, and IMQ-ETH were tested for L-929 and A375 cell killing using the MTT assay. After seeding, cells were treated with Imiquimod, Blank-ETH, and IMQ-ETH for 48 hours. After that, they spent four hours in MTT. The cell viability percentage was calculated by dividing the treatment group absorbance by the control group. IC50 values were calculated using GraphPad Prism. [25]

In vitro cellular uptake studies

Rhodamine 6G (Rh6G)

A375 cells were grown in 24-well microplates for 24 hours to test ethosome penetration. They then received Rhodamine 6G (Rh6G) and ethosomes loaded with rhodamine (Rh6G-ETH) for 1, 3, and 6 hours. After removing the growth media, the cells were fixed with PFA for 20 minutes and washed twice with PBS. After fixing, the cells were examined under a fluorescence microscope. [26]

Assay for cell viability of live and dead cells
A375 cells were placed in a 24-well plate at a density of 5 x 10^4 cells per well and incubated overnight. For 48 hours, we gave them Blank-Ethosome and varied Imiquimod and IMQ-Ethosome IC50 doses. After treatment, we fixed the cells with 4% PFA for 20 minutes and rinsed them with PBS. Fixed cells were stained for 30 minutes with a 5 µg/ml solution of ethidium bromide (EB) and acridine orange (AO). After incubation, we examined the cells with a 10x fluorescence microscope. [27]

Staining with DAPI (4',6-diamidino-2-phenylindole)
Overnight-grown A375 cells at 1 x 105 cells/well in a 12-well culture plate were used for adhesion. IMQ and IMQ-ETH IC50 dosages were then applied to cells for 48 hours. Following 48 hours of PBS washing, cells were fixed with 4% PFA for 20 minutes. After fixation, cells were treated with 0.1 µg/ml DAPI in PBS for 10 minutes. After washing the cells with PBS, a 40x fluorescent microscope was utilized to detect apoptosis-related morphological alterations.[28]

Preparation of Imiquimod loaded Ethosomal gel
The enhanced IMQ-ETH formulations were added to carbopol gel to make Ethosomal gel skin-safe. For a transparent dispersion, carbopol® 980NF was constantly spun in water at 500 rpm. To hydrate and swell, the dispersion was left overnight. Gentle stirring was done with the optimum IMQ-ETH and carbopol dispersion. Adding triethanolamine to carbopol dispersion created a vesicular gel. Instead of IMQ-ETH, the carbopol dispersion was mixed with Imiquimod solution to form the basic gel. [29]

Characterization of IMQ-loaded Ethosomal gels
We checked the ethosomal gel compositions' color, consistency, and pH with a benchtop pH meter. At 25°C, a Brookfield viscometer measured viscosity. We tested gel extrusion and spreadability. We sonicated the gel after shaking it with methanol to dissolve the medicine. We next filtered and HPLC-analyzed the solution to determine drug content. [30]

In vitro investigations of skin permeability and deposition
In vitro experiments of ethosomal gel penetration and skin settlement employed the same procedure.

3. RESULT AND DISCUSSION

Formulation of Imiquimod Ethosome
Imiquimod ethosomes were formulated via a two-step method involving thin-film hydration and sonication. Optimization was done using response surface methodology (Design-Expert software), considering phospholipid 90G, ethanol, and propylene glycol as independent variables, and vesicle size, entrapment efficiency, and flux as responses.

Optimization of formulation parameter using response surface methodology.
Vesicle Size (B1): Ranged 99.48–159.29 nm. Increased ethanol and phospholipid reduced size due to bilayer fluidization and steric stabilization, respectively. Propylene glycol had minimal effect.

Entrapment Efficiency (B2): Ranged 51.22–87.47%. Increased phospholipid and moderate ethanol improved entrapment; excessive ethanol decreased it. Propylene glycol showed slight positive influence.

Flux (B3): Ranged 0.39–1.67 µg/cm²/h. Higher ethanol enhanced flux; excessive phospholipid reduced it. Propylene glycol showed marginal improvement.

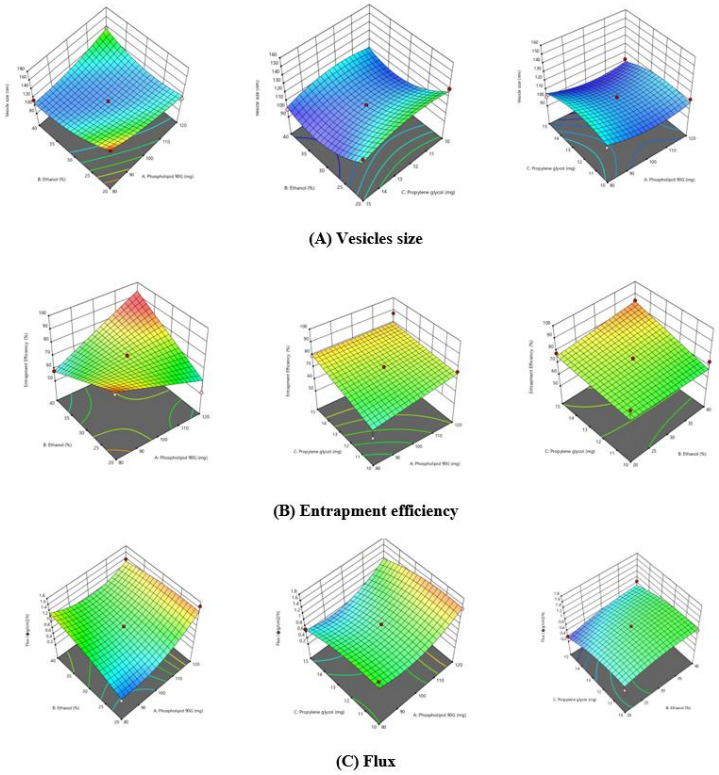

(A) Vesicles size

(B) Entrapment efficiency

(C) Flux

Figure_1: Impact of independent variables on dependent variables such as (A) vesicles size (B) entrapment efficiency and (C) flux in 3D

Characterization of ethosomes

Ethosomes morphology

IMQETH-3 (Red Curve) has the highest peak intensity, indicating a more uniform size distribution with smaller vesicles (~100 nm).

IMQETH-10 (Green Curve) has as lightly broader distribution with vesicles around 120nm.

IMQETH-14 (Blue Curve) has the largest vesicle size (~140 nm) and the broadest distribution. Since **smaller vesicle size and high intensity indicate better skin penetration**, **IMQETH-3** appears to be the best formulation for gel formation, ensuring efficient drug delivery**.**

Formulation Batches Code	Independent Factor Variable			Dependent Response Variable		
	A_1 Phospholipid 90G (mg)	**A_2 Ethanol (%)**	**A_3 Propylene glycol (mg)**	**B_1 Vesicle size (nm)**	**B_2 Entrapment Efficiency (%)**	**B_3 Flux (µg/cm2/h)**
IMQETH-1	**100**	**30**	5	**110.21**	**51.22**	**1.67**
IMQETH-2	**120**	**20**	5	**106.43**	**73.82**	**0.96**
IMQETH-3	**100**	**20**	2.5	**101.88**	**87.47**	**0.97**
IMQETH-4	**80**	**30**	2.5	**114.25**	**58.21**	**1.16**
IMQETH-5	**80**	**40**	5	**112.32**	**76.38**	**1.49**
IMQETH-6	**120**	**30**	7.5	**122.57**	**78.25**	**0.39**
IMQETH-7	**120**	**30**	2.5	**105.32**	**74.26**	**0.94**
IMQETH-8	**100**	**40**	2.5	**100.97**	**79.24**	**0.71**
IMQETH-9	**100**	**30**	5	**130.34**	**79.21**	**0.61**
IMQETH-10	**100**	**20**	7.5	**99.48**	**84.79**	**0.87**
IMQETH-11	**100**	**30**	5	**109.89**	**56.83**	**1.28**
IMQETH-12	**80**	**20**	5	**159.29**	**83.96**	**0.47**
IMQETH-13	**120**	**40**	5	**108.14**	**75.63**	**0.94**
IMQETH-14	**100**	**40**	7.5	**136.52**	**85.43**	**1.39**
IMQETH-15	**80**	**30**	7.5	**107.41**	**75.06**	**0.94**

Table_1: Response of Imiquimod ethosomal formulations obtained from Box Behnken design

Studies on skin penetration and deposition

The research investigated the transdermal permeation of Imiquimod from ethosome formulations across rat abdominal skin via a Franz diffusion cell. The cumulative quantity of Imiquimod that permeated through the skin varied from 48.35 ± 2.10 to 196.76 ± 3.25 µg/cm². The permeation flow augmented with the concentration of ethanol. The optimised ethosomal formulation IMQETH-3 exhibited a markedly greater cumulative quantity of Imiquimod compared to Imiquad Cream.

Formulation	Cumulative amount permeated (µg/cm²)	Permeation flux J(µg/cm²/h)	Permeability Coefficient Kp (cm/h)	Enhancement Ratio (ER)	Amount Deposited (µg/cm²)
IMQETH-1	48.35 ± 2.10	1.21 ± 0.08	2.48×10^{-3}	1.25	8.52 ± 0.21
IMQETH-2	67.94 ± 3.14	1.95 ± 0.05	3.12×10^{-3}	1.60	9.84 ± 0.18
IMQETH-3	174.56 ± 3.05	4.01 ± 0.09	7.94×10^{-3}	4.20	18.21 ± 0.45
IMQETH-4	59.33 ± 2.88	1.68 ± 0.07	2.96×10^{-3}	1.45	10.37 ± 0.31
IMQETH-5	78.44 ± 2.63	2.32 ± 0.04	3.87×10^{-3}	1.80	11.29 ± 0.24
IMQETH-6	85.67 ± 3.22	2.66 ± 0.06	4.45×10^{-3}	2.00	13.14 ± 0.30
IMQETH-7	91.11 ± 3.88	2.78 ± 0.09	4.60×10^{-3}	2.10	13.76 ± 0.29
IMQETH-8	106.34 ± 4.11	3.21 ± 0.07	5.45×10^{-3}	2.55	14.90 ± 0.26
IMQETH-9	61.77 ± 3.65	1.75 ± 0.05	3.10×10^{-3}	1.35	9.43 ± 0.34
IMQETH-10	189.22 ± 2.97	4.26 ± 0.11	8.33×10^{-3}	4.45	19.04 ± 0.52
IMQETH-11	69.88 ± 3.10	2.02 ± 0.06	3.42×10^{-3}	1.60	11.38 ± 0.35
IMQETH-12	77.53 ± 3.28	2.39 ± 0.07	4.01×10^{-3}	1.85	11.84 ± 0.29
IMQETH-13	88.01 ± 3.17	2.70 ± 0.05	4.64×10^{-3}	2.05	12.66 ± 0.33
IMQETH-14	196.76 ± 3.25	4.38 ± 0.08	8.75×10^{-3}	4.60	20.12 ± 0.48
IMQETH-15	66.40 ± 2.85	1.94 ± 0.06	3.25×10^{-3}	1.55	9.91 ± 0.27
Imiquad Cream (Glenmark)	89.39 ± 3.15	2.91 ± 0.08	4.01×10^{-3}	2.07	13.84 ±0.37

Table_2: Skin permeation of different Imiquimod formulations across the rat skin

Skin penetration efficiency of Ethosomal systems

Fluorescence photographs of the rat skin after 6 h treatment with Rh6G-IMQETH-3, and rhodamine-6G solution (control) are shown in Figure_2. The Rh6G solution showed fluorescence confined only to the superficial SC layer. In contrast to this, a fairly uniform bright fluorescence throughout the SC, epidermis, and dermis was observed after the treatment with Rh6G-IMQETH-3. Furthermore, the fluorescent area in the rat skin after the application with Rh6G-IMQETH-3 was also higher than that of Control Rh6G Solution provided in figure_2.

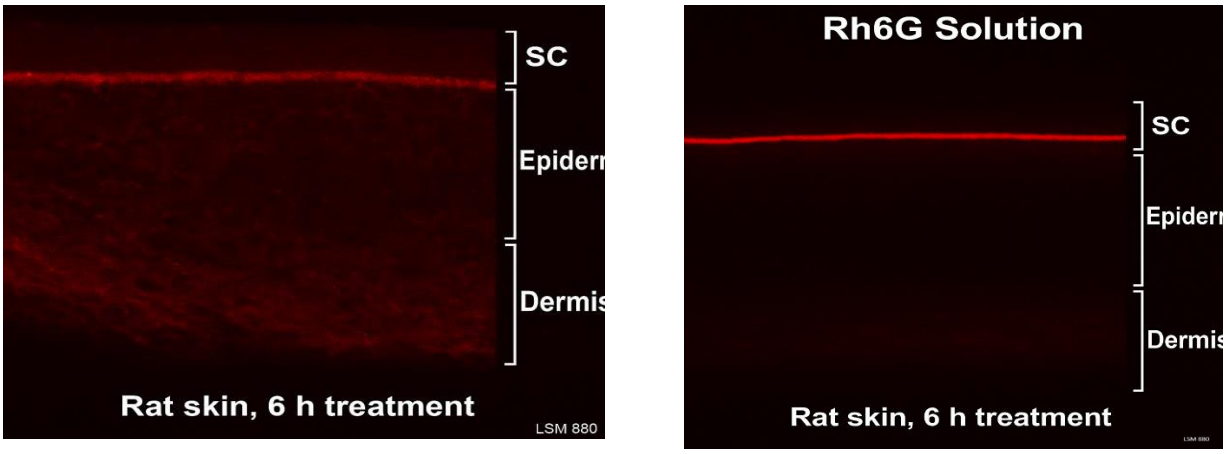

(A) **(B)**

Figure_2: Fluorescence photomicrographs of rat skin after 6h application of (A) rhodamine 6G loaded ethosomes and (B) rhodamine-6G solution

Characterization Freeze drying product by DSC, FTIR and XRD:

Pure Imiquimod showed a sharp endothermic peak at 291°C, indicating its crystalline nature. Blank Ethosomes showed no such peak, confirming their amorphous matrix. Imiquimod-loaded Ethosomes lacked the melting peak of pure Imiquimod, indicating molecular dispersion or amorphization of the drug within the vesicles, confirming stable entrapment without thermal degradation. Pure Imiquimod displayed sharp crystalline peaks. Blank Ethosomes showed broad, diffused peaks characteristic of amorphous materials. Imiquimod-loaded Ethosomes (IMQ-ETH-3) exhibited reduced or absent drug peaks, confirming transformation of Imiquimod from crystalline to amorphous/molecularly dispersed form within the formulation, enhancing solubility and stability. Blank Ethosomes showed characteristic peaks of Phospholipon® 90G. Imiquimod-loaded Ethosomes showed similar peaks with diminished or missing Imiquimod-specific peaks, indicating successful drug encapsulation and possible molecular dispersion within the ethosomal bilayer provided in figure_3.

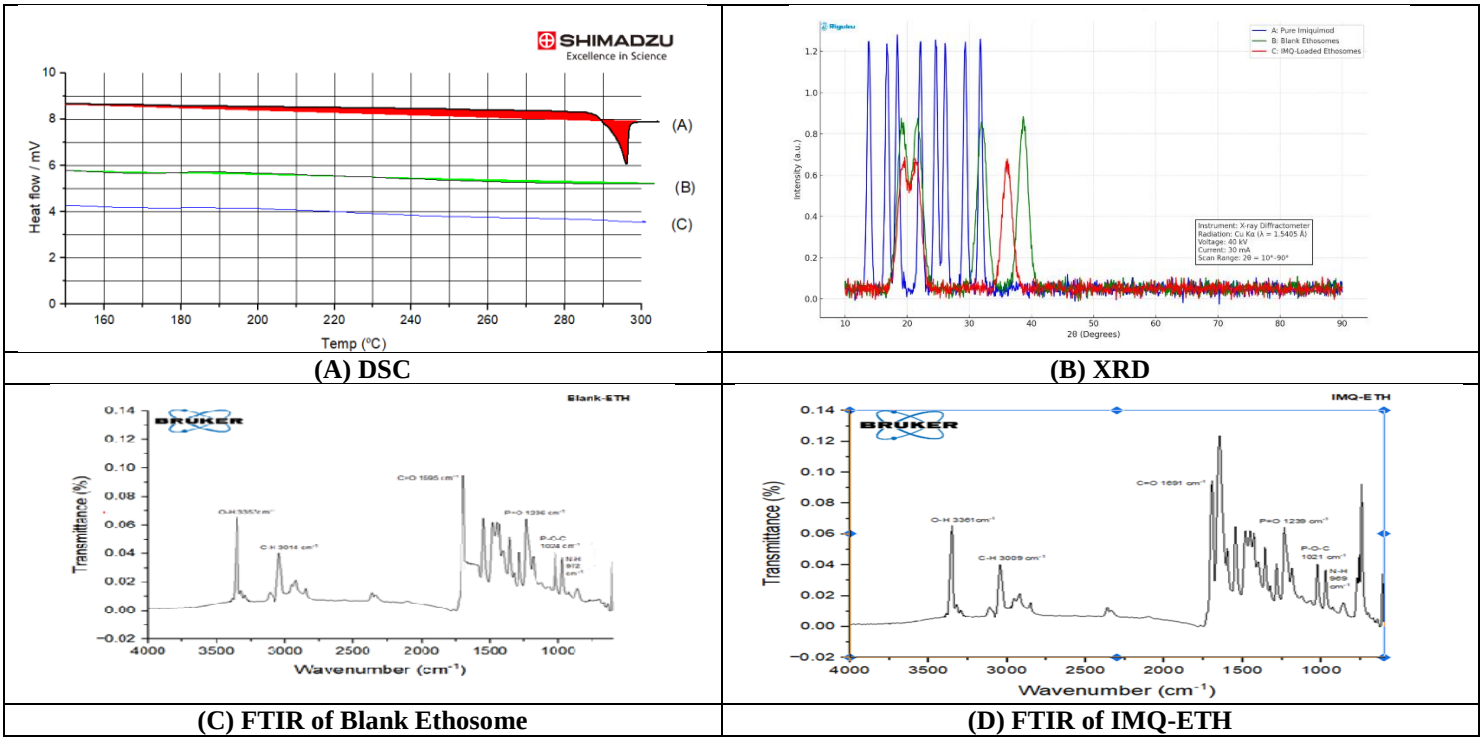

(A) DSC | (B) XRD

(C) FTIR of Blank Ethosome | (D) FTIR of IMQ-ETH

Figure_3: DSC, FTIR, and XRD compatibility profiles of Imiquimod and its ethosomal formulation.

In vitro cellular culture investigations

Invitro cytotoxicity assay

The in vitro cytotoxicity of Imiquimod, Blank-Ethosomes, and IMQ-Ethosomes was evaluated against the A-375 cell line and L-929 murine fibroblasts utilising the MTT assay. Following a 48-hour incubation with Imiquimod, Blank-ETH, and IMQETH-3, Figures_4 depicted the viability percentages of both cell types. In comparison to untreated cells, the vitality of L-929 murine fibroblast cells exposed to doses (1.5–60µg/ml) of different formulations maintained roughly 92%. A375 cells subjected to Imiquimod, Blank-ETH, and IMQETH-3 demonstrated concentration-dependent cytotoxicity provided in figure_4.

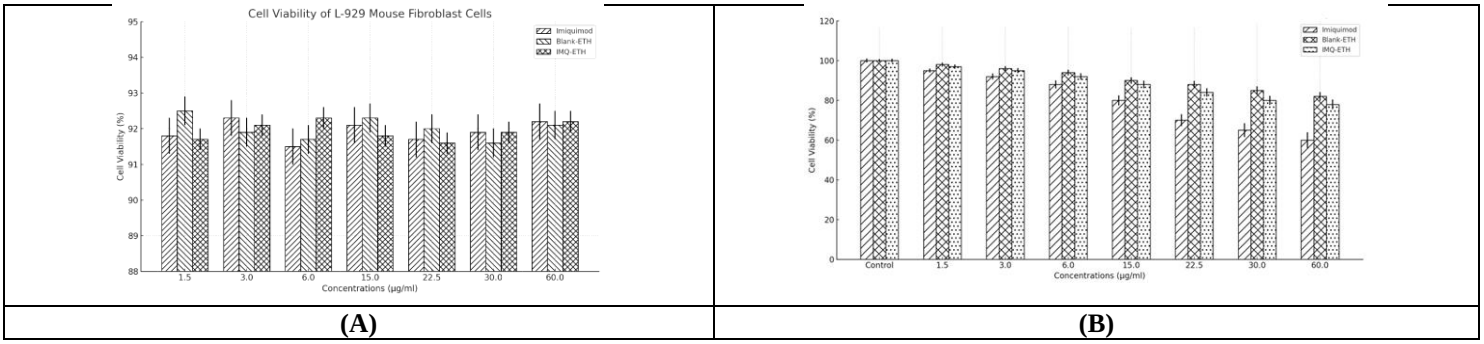

(A) | (B)

Figure_4: In vitro cytotoxicity effects of Imiquimod, Blank-ETH and IMQ-ETH on (A) L-929 and (B) A-375 cell line

***Invitro* cellular uptake studies**

Cellular uptake studies in A375 cells using rhodamine-6G (Rh6G) and Rh6G-loaded ethosomes (Rh6G-IMQETH-3) showed significantly higher fluorescence for the ethosomal group over 6 hours, indicating enhanced uptake. Free Rh6G showed negligible fluorescence after 3 hours.

Similarly, imiquimod and IMQETH-3 were tested. DAPI stained nuclei (blue) and imiquimod's green fluorescence revealed that IMQETH-3 achieved stronger cellular uptake and localized within both cytoplasm and nuclei, unlike pure imiquimod which showed weak fluorescence provided in figure_5.

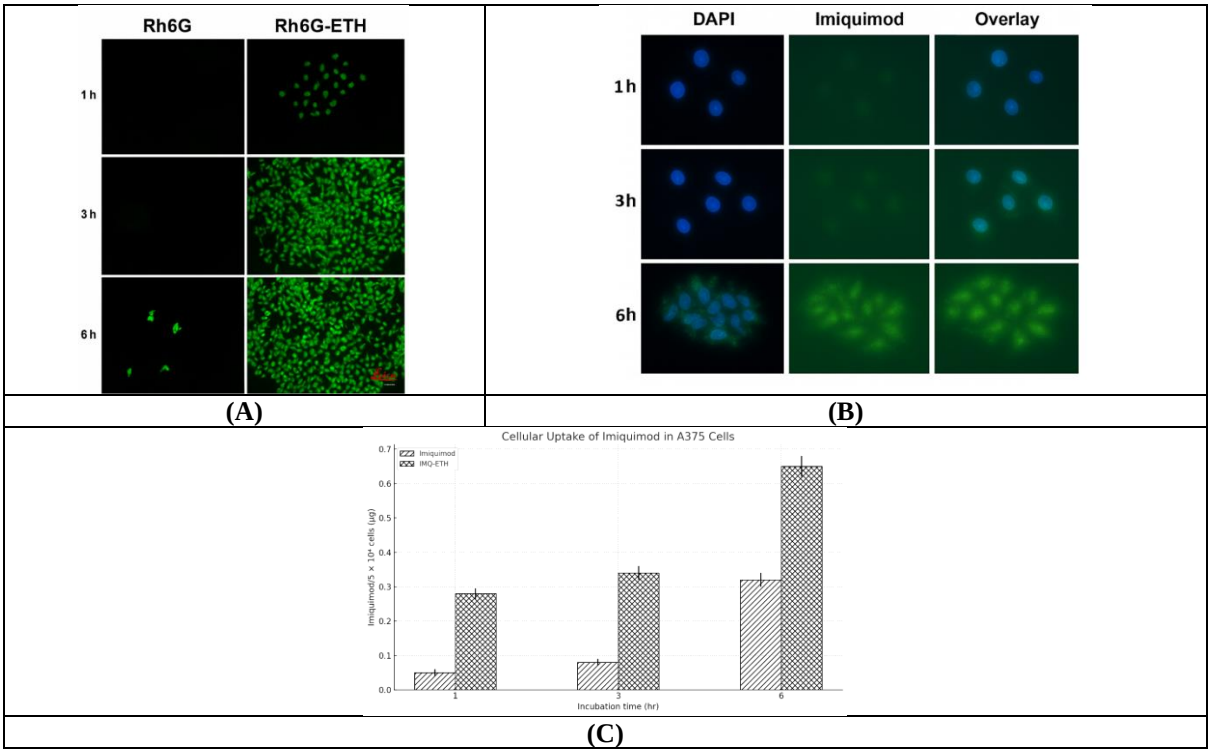

Figure_5: Cellular uptake studies in A375 cells: (A) Time-dependent uptake of Rh6G and Rh6G-ETH, (B) Fluorescence imaging of Imiquimod and IMQ-ETH uptake after 6 h, and (C) Quantitative uptake analysis

Live and dead cell assay

To distinguish between living and dead cells, dual acridine orange/ethidium bromide fluorescent labelling is utilized, which may be seen using a fluorescence microscope. The fluorescence microscopic pictures of A375 cells that were left untreated (control group) and cells that were exposed to blank-ETH and IMQETH-3 for 48 hours are displayed in Figure_6A The cells treated with Imiquimod and IMQETH-3 had a dark orange-red colour, whereas the cells in the untreated and blank-ETH treated groups appeared green with homogeneous intensity. In addition, there was also decreased number of cells in IMQ and IMQETH-3 treated groups compared to the control group provided in figure_6A.

DAPI staining

DAPI labelling was used to observe the apoptotic nuclear morphological alterations in A375 cells after they were treated with IMQ and its ethosomal formulations for 48 hours. The fluorescence microscopic images of untreated cells and cells treated with Blank-ETH Imiquimod and IMQETH-3 are displayed in Figure_6B. While the groups treated with IMQ and IMQETH-3 showed tiny nuclei with vivid chromatin condensation, blebbing, nuclear disintegration, and apoptotic body formation, the untreated cells and cells treated with Blank-ETH showed a normal intact nucleus with weak homogeneous blue staining provided in figure_6B.

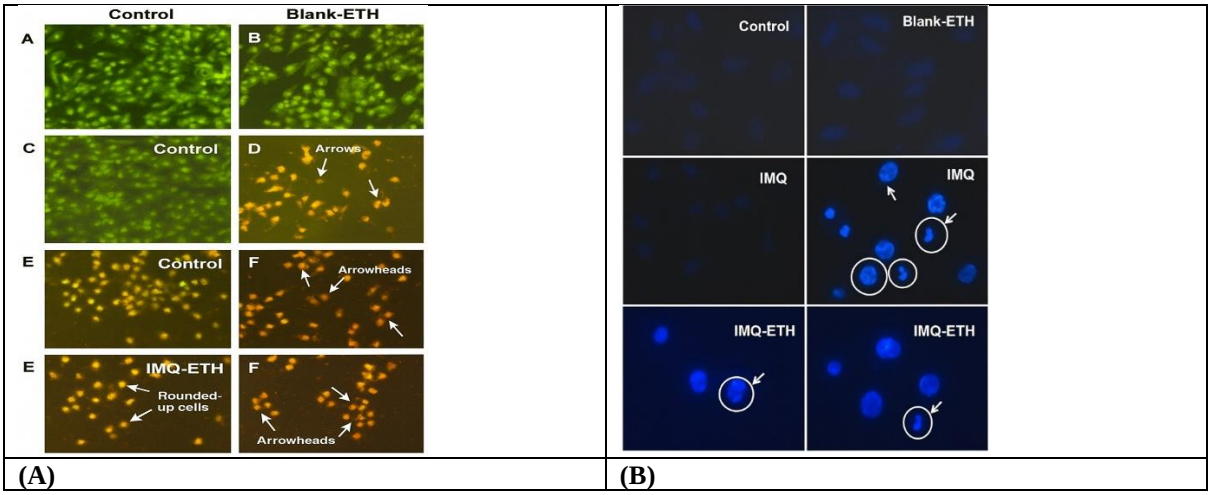

Figure_6: (A) Live and dead cell assay of A375 cells using AO and EB double staining with Blank-ETH, Imiquimod and IMQ-ETH for 48 h. (B) Apoptotic nuclear changes in A375 cells by DAPI staining. Cells were treated with Blank-ETH, Imiquimod and IMQ-ETH for 48 h.

Characterization of IMQ-loaded Ethosomal Gels

The prepared ethosomal gels of Imiquimod were evaluated for pH, viscosity, homogeneity, spreadability, extrudability and drug content. All the nanogel formulations have a smooth texture, good homogeneity and are free from gritty particles. The pH of all gels was found between 5.40 ± 0.03 and 5.45 ± 0.01. The viscosity of Imiquimod gel and IMQETH-3 gel was found to be 522.10 ± 12.18 and 710.25 ± 26.77 cPs respectively. The spreadability of Imiquimod gel and IMQETH-3 gel was found to be 3.7 ± 0.07 and 4.0 ± 0.06 gm.cm/sec. The extrudability of Imiquimod gel and IMQETH-3 gel was found to be 150.67 ± 8.14 and 168.45 ± 5.78 gm/cm². Imiquimod gel and IMQETH-3 gel were found to have a percent drug content of 98.85 ± 0.31 and 99.45 ± 0.22%.

In Vitro Skin Permeation and Skin Deposition Studies

Using Franz diffusion cells, the in vitro skin penetration and skin deposition capacity of Imiquimod ethosomal gels (IMQETH-3 Gel) over the rat skin was evaluated and contrasted with that of Imiquimod plain gel (IMQETH-3). The permeability coefficient, enhancement ratio, permeation flux, total amount of medication absorbed after a 24-hour period, and amount of drug deposited in the skin layers were all summarized in Table_3. When compared to IMQ-Gel, the cumulative amount of Imiquimod that permeated from IMQETH-3 Gel was substantially larger ($p<0.01$). Additionally, IMQETH-3 Gel's Imiquimod permeation flux was 5.19 times greater than IMQ-Gel's. It was discovered that the permeability coefficients of IMQ-Gel and IMQETH-3 Gel were 0.84×10^{-3} and 3.48×10^{-3} cm/h, respectively. Comparing IMQETH-3 to IMQ-Gel, significantly more Imiquimod was deposited in the skin ($p<0.05$).

Formulation	Cumulative amount permeated for 24hr(µg/cm^2)	Permeation flux(J, µg/cm2/h)	Permeability Coefficient (Kp,ratio cm/h)	Enhancement	Amount deposited (µg/cm2)
IMQ-ETH Gel	41.69 ± 1.38	1.48 ± 0.09	4.41 x 10-3	5.17	10.59 ± 0.17
IMQ-Gel	11.98 ± 3.09	0.71 ± 0.28	0.91 x 10-3	1.74	4.47 ± 1.09

Table_3: Skin permeation parameters of IMQ-ETH Gel and IMQ-Gel

Stability Studies

The IMQETH-3 gels were tested for their stability on storing them at three different temperature conditions of 4±2°C, 25±2°C and 40±2°C for three months. The gels were characterized for their physicochemical characteristics at the start of the stability study and end period. Table_4 summarizes the results of the stability study of Imiquimod-loaded ethosomal gel formulations. The colour and appearance remained unchanged for gel at three different temperatures over a three-month period. The % drug content for IMQETH-3 gels at three different storage conditions was observed to vary from 99.12 to 96.10 and pH varied from 5.34 to 5.30. The viscosity of IMQETH-3 gel changed from 694.35 to 683.15 cPs.

(a) IMQ-ETH gel	
Storage condition	

	4± 2 °C			25± 2 °C			40± 2 °C		
Time	**pH**	**Viscosity**	**% Drug content**	**pH**	**Viscosity**	**% Drug content**	**pH**	**Viscosity**	**% Drug content**
Initial	5.31 ± 0.03	701.39 ± 24.37	99.6	5.49 ± 0.03	704.89 ± 24.37	99.2	5.34 ± 0.03	703.08 ± 24.37	99.7
Three Month	5.29 ± 0.02	699.87 ± 21.37	99.01 ± 0.19	5.35 ±0.01	702.62 ±20.78	98.87 ± 0.19	5.31 ± 0.03	705.21 ± 21.51	97.43 ± 0.67

Table_4: Stability of IMQ-ETH gel at different storage conditions as per ICH Q1A guidelines.

4. CONCLUSION

The present study successfully developed an ethosomal gel formulation of Imiquimod for the topical treatment of skin cancer, addressing limitations of conventional therapies such as poor skin penetration and systemic side effects. Preformulation studies confirmed the crystalline and hydrophobic nature of Imiquimod and its solubility in lactic acid and phosphatidylcholine, guiding the formulation approach. Analytical methods using UV and RP-HPLC were developed and validated, demonstrating high accuracy, precision, and sensitivity for drug quantification.

Ethosomal formulations were prepared by a modified cold method and optimized using Box-Behnken design. Among the formulations, IMQETH-3 showed the highest entrapment efficiency (87.47%), IMQETH-10 had the smallest vesicle size (99.48 nm), and IMQETH-14 exhibited superior drug permeation. Transmission electron microscopy confirmed the nano-sized, spherical morphology of the vesicles. In vitro skin permeation studies revealed that the ethosomal gel significantly outperformed both plain gel and commercial cream in terms of drug delivery through the skin.

Fluorescence microscopy demonstrated enhanced penetration of the ethosomes into deeper skin layers. Cell culture studies using A375 melanoma cells and L929 fibroblast cells showed that the ethosomal formulation was non-toxic to normal cells but highly effective against cancer cells. Cellular uptake studies, MTT assay, and DAPI staining confirmed efficient drug entry into the nucleus and apoptosis induction. DNA fragmentation and flow cytometry further supported the apoptotic effect, while colony inhibition and morphological changes highlighted reduced cancer cell growth and replication.

The optimized formulation was incorporated into a gel using Carbopol 934, resulting in a stable, skin-compatible product with appropriate pH (5.4), smooth texture, good spreadability, and high drug content. The IMQETH-3 gel demonstrated five times greater skin permeation and retention compared to the plain gel. Stability studies over three months showed consistent pH, viscosity, and drug content, confirming the gel's suitability for long-term storage.

In conclusion, the Imiquimod-loaded ethosomal gel developed in this study is safe, stable, and significantly more effective in delivering the drug to deeper skin layers than conventional formulations. It shows great promise as a targeted therapy for superficial skin cancers like basal cell carcinoma and holds potential for future clinical application and commercial development.

Acknowledgments: None
Conflict of interest: The authors declare no conflict of interest.
Funding sources: None.

REFERENCES:

[1] Ma, M.; Wang, J.; Guo, F.; Liu, M.; Tan, F.; Li, N. Development of Nanovesicular Systems for Dermal Imiquimod Delivery: Physicochemical Characterization and in Vitro/in Vivo Evaluation. Journal of Materials Science: Materials in Medicine 2015, 26 (6). https://doi.org/10.1007/s10856-015-5524-1.
[2] International council for harmonisation of technical requirements for pharmaceuticals for human use ich harmonised guideline validation of analytical procedures. https://database.ich.org/sites/default/files/ICH_Q2-R2_Document_Step2_Guideline_2022_0324.pdf.

[3] Dianzani, C.; Zara, G. P.; Maina, G.; Pettazzoni, P.; Pizzimenti, S.; Rossi, F.; Gigliotti, C. L.; Ciamporcero, E. S.; Daga, M.; Barrera, G. Drug Delivery Nanoparticles in Skin Cancers. BioMed Research International 2014, 2014, 1–13. https://doi.org/10.1155/2014/895986.
[4] Dias, M. F.; Figueiredo, B. C. P. de; Teixeira-Neto, J.; Guerra, M. C. A.; Fialho, S. L.; Silva Cunha, A. In Vivo Evaluation of Antitumoral and Antiangiogenic Effect of Imiquimod-Loaded Polymeric Nanoparticles. Biomedicine & Pharmacotherapy 2018, 103, 1107–1114. https://doi.org/10.1016/j.biopha.2018.04.079.
[5] Pandey, M.; Choudhury, H.; Gorain, B.; Tiong, S. Q.; Wong, G. Y. S.; Chan, K. X.; They, X.; Chieu, W. S. Site-Specific Vesicular Drug Delivery System for Skin Cancer: A Novel Approach for Targeting. Gels 2021, 7 (4), 218. https://doi.org/10.3390/gels7040218.
[6] Waqar, M. A.; Mubarak, N.; Khan, A. M.; Zaib, M.; Shoaib, Q.-A.; Alvi, A. S.; Dua-E-Zahra, S. Ethosomes as a New Frontier and Revolutionary Approach for Targeted Skin Cancer Therapy. International Journal of Polymeric Materials and Polymeric Biomaterials 2025, 1–22. https://doi.org/10.1080/00914037.2025.2493916.
[7] Gupta, V.; Chuttani, K.; Mishra, A. K.; Trivedi, P. Topical Delivery of Fluorescence (6-Cf) Labeled and Radiolabeled (99m-Tc) Cisplatin and Imiquimod by a Dual Drug Delivery System. Journal of Labelled Compounds and Radiopharmaceuticals 2014, 57 (6), 425–433. https://doi.org/10.1002/jlcr.3201.
[8] Ma, M.; Wang, J.; Guo, F.; Liu, M.; Tan, F.; Li, N. Development of Nanovesicular Systems for Dermal Imiquimod Delivery: Physicochemical Characterization and in Vitro/in Vivo Evaluation. Journal of Materials Science: Materials in Medicine 2015, 26 (6). https://doi.org/10.1007/s10856-015-5524-1.
[9] Shinde, P.; Page, A.; Bhattacharya, S. Ethosomes and Their Monotonous Effects on Skin Cancer Disruption. Frontiers in Nanotechnology 2023, 5. https://doi.org/10.3389/fnano.2023.1087413.
[10] Dianzani, C.; Zara, G. P.; Maina, G.; Pettazzoni, P.; Pizzimenti, S.; Rossi, F.; Gigliotti, C. L.; Ciamporcero, E. S.; Daga, M.; Barrera, G. Drug Delivery Nanoparticles in Skin Cancers. BioMed Research International 2014, 2014, 1–13. https://doi.org/10.1155/2014/895986.
[11] Waqar, M. A.; Mubarak, N.; Khan, A. M.; Zaib, M.; Shoaib, Q.-A.; Alvi, A. S.; Dua-E-Zahra, S. Ethosomes as a New Frontier and Revolutionary Approach for Targeted Skin Cancer Therapy. International Journal of Polymeric Materials and Polymeric Biomaterials 2025, 1–22. https://doi.org/10.1080/00914037.2025.2493916.
[12] Petrová, E.; Chvíla, S.; Balouch, M.; Štěpánek, F.; Zbytovská, J. Nanoformulations for Dermal Delivery of Imiquimod: The Race of "Soft" against "Hard." International Journal of Pharmaceutics 2023, 648, 123577. https://doi.org/10.1016/j.ijpharm.2023.123577.
[13] Seenivasan, R.; Halagali, P.; Nayak, D.; Tippavajhala, V. K. Transethosomes: A Comprehensive Review of Ultra-Deformable Vesicular Systems for Enhanced Transdermal Drug Delivery. AAPS PharmSciTech 2025, 26 (1). https://doi.org/10.1208/s12249-024-03035-x.
[14] Abpeikar, Z.; Safaei, M.; Akbar Alizadeh, A.; Goodarzi, A.; Hatam, G. The Novel Treatments Based on Tissue Engineering, Cell Therapy and Nanotechnology for Cutaneous Leishmaniasis. International Journal of Pharmaceutics 2023, 633, 122615. https://doi.org/10.1016/j.ijpharm.2023.122615.
[15] Zang, X.; Kagan, L. Physiologically-Based Modeling and Interspecies Prediction of Cisplatin Pharmacokinetics. Journal of Pharmaceutical Sciences 2024, 113 (1), 158–166. https://doi.org/10.1016/j.xphs.2023.10.022.
[16] Abd El-Alim, S. H.; Kassem, A. A.; Basha, M.; Salama, A. Comparative Study of Liposomes, Ethosomes and Transfersomes as Carriers for Enhancing the Transdermal Delivery of Diflunisal: In Vitro and in Vivo Evaluation. International Journal of Pharmaceutics 2019, 563, 293–303. https://doi.org/10.1016/j.ijpharm.2019.04.001.
[17] Limsuwan, T.; Boonme, P.; Khongkow, P.; Amnuaikit, T. Ethosomes of Phenylethyl Resorcinol as Vesicular Delivery System for Skin Lightening Applications. BioMed Research International 2017, 2017, 1–12. https://doi.org/10.1155/2017/8310979.
[18] Shukla, R.; Tiwari, G.; Tiwari, R.; Rai, A. K. Formulation and Evaluation of the Topical Ethosomal Gel of Melatonin to Prevent UV Radiation. Journal of Cosmetic Dermatology 2019. https://doi.org/10.1111/jocd.13251.
[19] Bragagni, M.; María Esther Gil-Alegre; Mura, P.; Cirri, M.; Ghelardini, C.; Di, L. Improving the Therapeutic Efficacy of Prilocaine by PLGA Microparticles: Preparation, Characterization and in Vivo Evaluation. International Journal of Pharmaceutics 2018, 547 (1-2), 24–30. https://doi.org/10.1016/j.ijpharm.2018.05.054.
[20] Touitou, E.; Dayan, N.; Bergelson, L.; Godin, B.; Eliaz, M. Ethosomes — Novel Vesicular Carriers for Enhanced Delivery: Characterization and Skin Penetration Properties. Journal of Controlled Release 2000, 65 (3), 403–418. https://doi.org/10.1016/s0168-3659(99)00222-9.
[21] Ilaria Andreana; Bincoletto, V.; Maela Manzoli; Rodà, F.; Giarraputo, V.; Milla, P.; Berlier, G.; Stella, B. Freeze Drying of Polymer Nanoparticles and Liposomes Exploiting Different Saccharide-Based Approaches. Materials 2023, 16 (3), 1212–1212. https://doi.org/10.3390/ma16031212.
[22] Ma, H.; Guo, D.; Fan, Y.; Wang, J.; Cheng, J.; Zhang, X. Paeonol-Loaded Ethosomes as Transdermal Delivery Carriers: Design, Preparation and Evaluation. Molecules 2018, 23 (7), 1756. https://doi.org/10.3390/molecules23071756.

[23] Niu, J.; Yuan, M.; Li, H.; Liu, Y.; Wang, L.; Fan, Y.; Zhang, Y.; Liu, X.; Li, L.; Zhang, J.; Zhao, C. Pentapeptide Modified Ethosomes for Enhanced Skin Retention and Topical Efficacy Activity of Indomethacin. Drug Delivery 2022, 29 (1), 1800–1810. https://doi.org/10.1080/10717544.2022.2081739.

[24] Majidi, F. S.; Mohammadi, E.; Mehravi, B.; Nouri, S.; Ashtari, K.; Neshasteh-riz, A. Investigating the Effect of near Infrared Photo Thermal Therapy Folic Acid Conjugated Gold Nano Shell on Melanoma Cancer Cell Line A375. Artificial Cells, Nanomedicine, and Biotechnology 2019, 47 (1), 2161–2170. https://doi.org/10.1080/21691401.2019.1593188.

[25] Liao, W.; Xiang, W.; Wang, F.-F.; Wang, R.; Ding, Y. Curcumin Inhibited Growth of Human Melanoma A375 Cells via Inciting Oxidative Stress. Biomedicine & Pharmacotherapy 2017, 95, 1177–1186. https://doi.org/10.1016/j.biopha.2017.09.026.

[26] Lee, W.-H.; Bebawy, M.; Loo, C.-Y.; Luk, F.; Mason, R. S.; Ramin Rohanizadeh. Fabrication of Curcumin Micellar Nanoparticles with Enhanced Anti-Cancer Activity. Journal of Biomedical Nanotechnology 2014, 11 (6), 1093–1105. https://doi.org/10.1166/jbn.2015.2041.

[27] Kulhari, H.; Pooja, D.; Singh, M. K.; Kuncha, M.; Adams, D. J.; Sistla, R. Bombesin-Conjugated Nanoparticles Improve the Cytotoxic Efficacy of Docetaxel against Gastrin-Releasing but Androgen-Independent Prostate Cancer. Nanomedicine 2015, 10 (18), 2847–2859. https://doi.org/10.2217/nnm.15.107.

[28] Halder, B.; Singh, S.; Thakur, S. S. Correction: Withania Somnifera Root Extract Has Potent Cytotoxic Effect against Human Malignant Melanoma Cells. PLOS ONE 2015, 10 (10), e0141053.

[29] Aggarwal, N.; Goindi, S. Dermatopharmacokinetic and Pharmacodynamic Evaluation of Ethosomes of Griseofulvin Designed for Dermal Delivery. Journal of Nanoparticle Research 2013, 15 (10). https://doi.org/10.1007/s11051-013-1983-9.

[30] Ahad, A.; Al-Saleh, A. A.; Al-Mohizea, A. M.; Al-Jenoobi, F. I.; Raish, M.; Yassin, A. E. B.; Alam, M. A. Pharmacodynamic Study of Eprosartan Mesylate-Loaded Transfersomes Carbopol® Gel under Dermaroller® on Rats with Methyl Prednisolone Acetate-Induced Hypertension. Biomedicine & Pharmacotherapy 2017, 89, 177–184. https://doi.org/10.1016/j.biopha.2017.01.164.